

3D velocity distribution functions of heavy ions and kinetic properties of O^{6+} at 1 AU

L. Berger^{*}, R. F. Wimmer-Schweingruber^{*} and G. Gloeckler[†]

^{*}*Extraterrestrial Physics, Institute for Experimental and Applied Physics, Christian-Albrechts-University Kiel, Germany*

[†]*Department of Atmospheric, Oceanic and Space Sciences, University of Michigan, Ann Arbor, Michigan 48109-2143, USA*

Abstract. The kinetic properties of the solar wind are a result of complex interactions in the solar corona and interplanetary space. So far, observations of Velocity Distribution Functions (VDFs) of solar wind heavy ions have been solely 1D. They are known to exhibit non-thermal features, but because they are 1D projections of the 3D velocity phase space it is difficult to interpret them properly. Based on 3D observations of protons and alpha particles from Helios, we have set up a model for heavy-ion VDFs. In it, the magnetic field vector plays a crucial role by defining the symmetry axis of the VDFs. A thermal anisotropy $T_{\parallel}/T_{\perp} \neq 1$ and a beam drifting along the magnetic field vector at a relative speed of approximately the Alfvén speed are included. The modeled VDFs are analysed using a virtual detector and then compared with data from the Solar Wind Ion Composition Spectrometer (SWICS) on the Advanced Composition Explorer (ACE). Our observations give evidence for the existence of heavy-ion beams. The projection of these beams can explain observed differential streaming. We present in-situ measurements and derived kinetic properties of O^{6+} at 1 AU.

Keywords: heavy ions, differential streaming, velocity distribution functions

PACS: 96.50.Ci

INTRODUCTION

From Helios measurements the 3D VDFs of protons (and alpha particles) are known to be highly non-thermal [1, 2]. They consist of a dense core and a dilute beam that is drifting along the local magnetic-field vector with approximately the local Alfvén velocity. These distributions can be modeled by two bi-Maxwellians [3]. To explain the beam formation and the observed thermal anisotropies, theoretical approaches simulating wave-particle interaction show promising results [4]. For heavy solar wind ions the shape of the 3D VDFs is unknown but it has to be assumed to interpret the 1D measurements. Commonly a single Maxwellian is assumed, although the measurements show pronounced non-thermal features. Consequently there is a need to improve our knowledge of the 3D shape of the VDFs of heavy ions to understand their evolution and to make such observations available to theoreticians and modelers.

To study the 3D VDFs of heavy ions we have set up a model of the Solar Wind Ion Composition Spectrometer (SWICS) that simulates the characteristics of the instrument. With this model we can calculate the expected shape of the 1D VDF for an input 3D VDF. Comparing the model calculations with observations, the characteristics of the 3D VDFs of heavy ions can be derived.

In this paper we present observational evidence for the existence of beams in the VDFs of O^{6+} in the fast solar

wind. These beams are more pronounced for O^{6+} than for protons and therefore cause a shift in the centre of mass velocity to higher velocities. In the usual assumption of a mono-Maxwellian VDF this shift will be interpreted as differential streaming of O^{6+} with respect to protons.

ANALYSIS

For our studies we used SWICS PHA data. SWICS velocity distributions were obtained using a maximum likelihood analysis technique that is based on Poissonian statistics [5]. Additionally MAG and SWEPAM level 2 data¹ have been used.

Based on proton observations [3] we have used two drifting bi-Maxwellians to model the 3D VDFs of heavy ions (s. Fig. 1). The distribution is placed in Sun-Earth frame of reference at a velocity v_C . The temperatures T_{\parallel} and T_{\perp} , and the drift velocity v_d between the two components are given in a magnetic-field vector based frame of reference. The intensity of the core and the beam component are given by n_C , and n_B respectively.

SWICS is a linear time-of-flight mass spectrometer with electrostatic deflection. From its measurements mass, charge, and total energy of incoming ions can be deter-

¹ <http://www.srl.caltech.edu/ACE/ASC/level2/index.html>

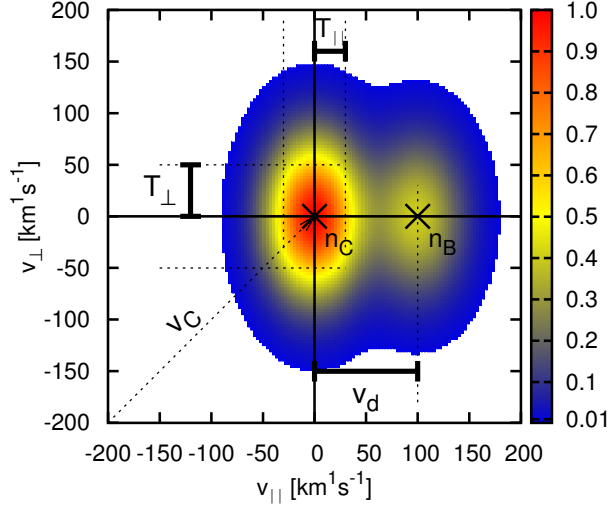


FIGURE 1. 3D-core-beam-model VDF and its parameters. The X-Axis v_{\parallel} is defined by the magnetic-field vector (always Sun-Earth pointing) and a rotational symmetry related to it. Relative intensity is colour-coded.

mined. Because only the total energy is determined, the measured distributions are 1D projections of the 3D velocity phase space.

We have set up a sophisticated model that simulates the characteristics of SWICS [5]. It incorporates the gyration and the orientation of the axis of rotation of the instrument as well as the instrumental efficiencies [6]. The model detector can be applied to an 3D VDF and calculates the corresponding 1D VDF. Figure 2 shows an example of a core-beam bi-Maxwellian distribution for two different magnetic field directions. The signature of a beam in the 1D distribution will depend strongly on the angle β between Sun-Earth line and the direction of the magnetic field vector. Only for small angles β a beam will be visible in the 1D projections (left-hand panel). If this angle is approximately the Parker angle the 1D distribution will look like a mono-Maxwellian with the right slope being raised (right-hand panel).

Observations

The 1D distributions we obtain from our model (s. lower panel of Fig. 2) have been compared to observations. We find that the core-beam distributions can reproduce the observations better than mono-Maxwellian distributions. Figure 3 shows an example of a comparison for the case of a small angle β between Sun-Earth line and magnetic field vector. The used parameters are listed in table 1.

At the top protons are shown. Observations (red boxes) and core-beam model (blue boxes) almost lie on top of

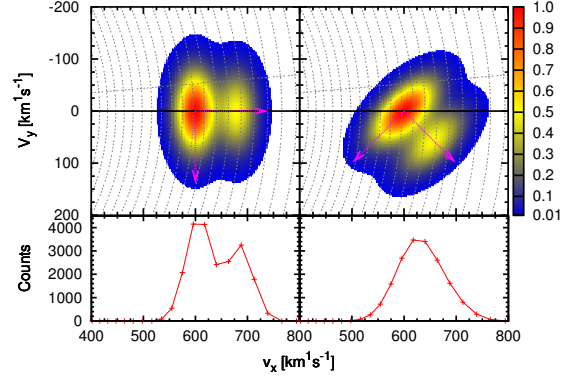


FIGURE 2. In the upper panels 2D cuts of 3D-core-beam VDFs are shown. X-axis is Sun-Earth pointing. Both distributions have the same parameters but the angle β between Sun-Earth line and magnetic-field vector is different (left : $\beta=0$ rad, right : $\beta=\pi/4$ rad). Magnetic-field coordinates are indicated by the magenta arrows. The grey segments of a circle indicate the phase space scan done by SWICS and the grey line indicates the orientation of the spacecraft. In the lower panels the corresponding 1D-VDFs are shown. The difference arising from different angles is clearly visible.

each other. The signatures of core and beam are clearly visible from the observations. The model parameters are in good agreement with proton observations from Helios [3]. Additionally a mono-Maxwellian model (magenta line) is shown. Obviously the agreement between model and observation is worse. The poor agreement of both models in the outer slopes potentially can be improved by the use of κ -functions (not further discussed in this paper).

In the middle alpha particles are shown. The signatures of core and beam are less visible from the observations (red crosses). This is due to the higher beam intensity $n_B/n_C=0.72$ that results in a broad plateau that can be reproduced by the core-beam model (blue crosses), the blue and red crosses almost lie on top of each other. Again the agreement of the mono-Maxwellian model (magenta line) is worse.

At the bottom O^{6+} (asterisks) is shown. The centre of the distribution ($600 \text{ km}^1\text{s}^{-1} < v < 700 \text{ km}^1\text{s}^{-1}$) looks similar to the distribution of alpha particles showing a plateau that cannot be reproduced by the mono-Maxwellian model (magenta line). The core-beam model (blue) with a beam that is more pronounced than the core $n_B/n_C=1.1$ can reproduce the observations (red). The centre of mass velocities v_{sw} for He^{2+} and O^{6+} are higher than for H^{1+} . This phenomenon is known as differential streaming. According to the core-beam model this difference in velocity is for one part due to a shift in the core velocity v_C and for another part due to different beam intensities n_B/n_C .

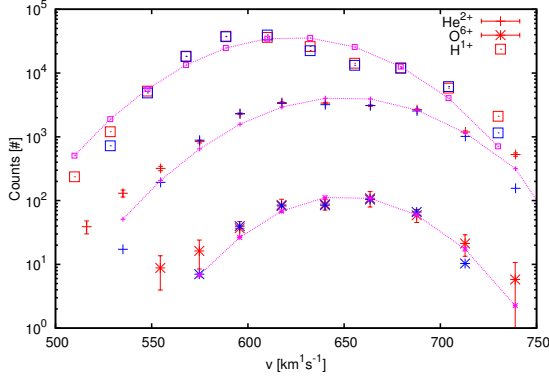


FIGURE 3. 12 minute observations (red symbols) of H^{1+} (top, boxes), He^{2+} (middle, crosses), and O^{6+} (lower, asterisks). Model calculations using mono-Maxwellian VDFs (magenta curves). In the centre of the distributions the core-beam model (blue) lies on top of the observations (red) and is reproducing the observations better than the mono-Maxwellian model.

TABLE 1. Model parameters. Velocities are in $km\ s^{-1}$, densities in cm^{-3} . Corresponding 1D distributions are shown in figure 3

	H^{1+}	He^{2+}	O^{6+}
DoY		120.77	
v_C	595	610	615
v_d	75	60	50
$v_{T\perp}$	40	45	40
$v_{T\parallel}$	25	26	20
n_B+n_C	$1.5 \cdot 10^0$	$9.3 \cdot 10^{-2}$	$6.3 \cdot 10^{-4}$
n_B/n_C	0.23	0.72	1.10
$\beta[rad]$		0.13	
v_{Alf}		58	
v_{sw}	615	642	646

DIFFERENTIAL STREAMING

For core-beam distributions we expect a dependence of the measured differential streaming on the angle β between Sun-Earth line and magnetic field direction as can be seen in the lower panel of figure 2. This is because the beams are drifting along the magnetic field vector but SWICS projects the 3D VDFs to Sun-Earth line.

We have analysed the differential streaming of O^{6+} with respect to protons in fast solar wind $v_{sw} > 600 km\ s^{-1}$ during quite times. Table 2 lists periods of quite time solar wind from which only times of fast solar wind were taken. We find that the observed differential streaming strongly depends on the angle β . Figure 4 shows the dependence of mean observed differential streaming on β . The four curves correspond to different subsets of data. The two curves labeled with no $\Delta\beta$ filter show the results for the whole data sample in 1 hour and 12 minutes resolution. Both show a trend that is more pronounced for 12

minute data. For the remaining two curves the data has been filtered using the condition that

$$\Delta\beta < 0.2 rad \quad (1)$$

where $\Delta\beta$ is the standard deviation of β within the time resolution of the data. In both cases the trend becomes more pronounced. This indicates that the shift in the centre of mass velocities of heavy ions is along the local magnetic field direction.

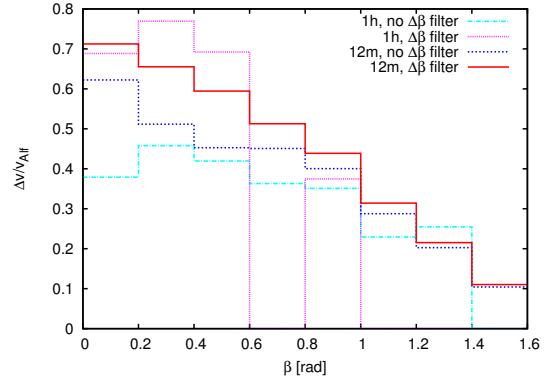


FIGURE 4. The dependence of the differential streaming of O^{6+} with respect to H^{1+} on β . 1 hour and 12 minutes data are compared. Additionally the influence of the variability of β within the measuring time is shown (s. text).

TABLE 2. Periods of quite time solar wind. Dates are in day of year 2007.

from	-	to	from	-	to
4.00	-	9.00	73.25	-	80.50
17.40	-	25.25	93.00	-	97.50
30.50	-	35.00	103.00	-	107.00
45.50	-	55.00	119.00	-	126.50
60.00	-	63.00	129.00	-	135.00
65.50	-	70.00	145.25	-	151.10

O^{6+} PARAMETERS

The fact that the observed differential streaming of O^{6+} depends on the direction of the magnetic field β allows for determine mean kinetic parameters of O^{6+} . For observations and model distributions we obtain differential streaming and thermal velocity by calculating the first and second order moments of the 1D VDFs. If we use core-beam VDFs and assume that the parameters v_C , v_d , n_B/n_C , $v_{T\perp}$, and $v_{T\parallel}$ may vary in time but are independent from β , we can compare model calculations with mean observed values. For a given set of parameters we can calculate the expected differential streaming and thermal velocities depending on β and compare them to mean observations. We used a Levenberg-Marquardt algorithm [7] to determine the parameters that reproduce

the observations best (s Figs. 5,6). The obtained parameter of O^{6+} are listed in Table 3. In contrast to protons the beams are strongly pronounced. The velocity of the core v_C equals the centre of mass velocity of the protons $v_{H^{1+}}$. Therefore the core is at rest in a solar wind frame of reference. In this frame of reference the beams drift with the local Alfvén velocity v_{Alf} along the magnetic field direction. The mean thermal anisotropy of core and beam is $T_{\perp}/T_{\parallel} = 1.52$.

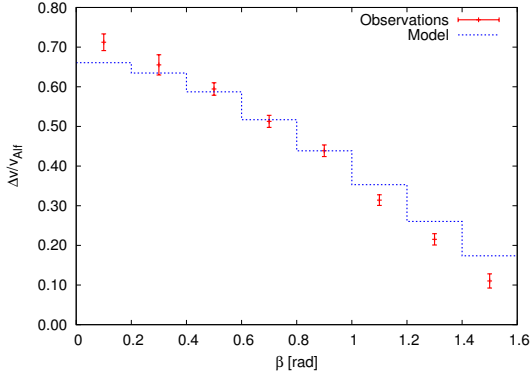


FIGURE 5. Differential streaming of O^{6+} depending on β are shown. Observed mean values are compared with model calculations using the parameters listed in table 3.

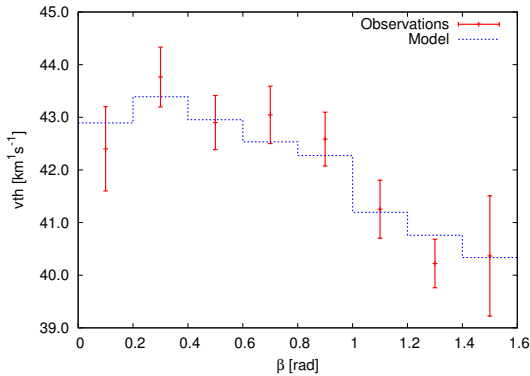


FIGURE 6. Thermal velocities of O^{6+} depending on β are shown. Observed mean values are compared with model calculations using the parameters listed in table 3.

TABLE 3. Mean parameters of O^{6+} at 1 AU. Velocities are in km s^{-1}

v_C	v_d	$v_{T\perp}$	$v_{T\parallel}$	n_B/n_C
$v_{H^{1+}}$	v_{Alf}	41.0	33.3	1.195

SUMMARY/CONCLUSIONS

In this paper we have addressed the microscopic kinetic state of heavy solar wind ions. We have shown that the assumption of 3D core-beam distributions similar to that

of protons are in agreement with ACE/SWICS observations of heavy ions. For fast solar wind O^{6+} a strong dependency of the observed differential streaming with respect to protons on the angle β between Sun-Earth line and magnetic field vector has been found. This is in close agreement with the expectations from core-beam VDFs. In this case the differential streaming is a shift in the centre of mass velocities caused by beams that are more pronounced for heavy ions than for protons. This shift pointing along the local magnetic field direction is then projected by SWICS to Sun-Earth line causing the dependency on β . In particular we found that the observed trend flattens with increasing variability of β within the time resolution of the data. This indicates that the VDFs are shaped locally out to 1 AU. The similar shape of heavy ion and proton VDFs indicates that the same processes are responsible. Finally we derived mean kinetic parameters of O^{6+} at 1 AU. Further studies including more ion species covering a wide range in mass and charge are suited to pinpoint the processes responsible for the kinetic evolution of solar wind ions.

ACKNOWLEDGMENTS

This work was supported, by the Deutsche Forschungsgemeinschaft DFG (Grant: WI2139/2).

REFERENCES

1. E. Marsch, R. Schwenn, H. Rosenbauer, K.-H. Mühllhäuser, W. Pilipp, and F. M. Neubauer, *Journal of Geophysical Research* **87**, 52–72 (1982).
2. E. Marsch, K.-H. Mühllhäuser, H. Rosenbauer, R. Schwenn, and F. M. Neubauer, *Journal of Geophysical Research* **87**, 35–51 (1982).
3. M. Heuer, and E. Marsch, *Journal of Geophysical Research* **112** (2007).
4. J. A. Araneda, E. Marsch, and A. F. Viñas, *PRL* **100** (2008).
5. L. Berger, *Velocity Distribution Functions of Heavy Ions in the Solar Wind at 1 AU*, Ph.D. thesis, IEAP, CAU-Kiel, Germany (2008).
6. M. Köten, *An improved efficiency model for ACE/SWICS - Determination of the carbon isotopic ratio $^{13}C/^{12}C$ in the solar wind from ACE/SWICS measurements*, Ph.D. thesis, Christian Albrechts Universität, Kiel (2009).
7. W. H. Press, S. A. Teukolsky, W. T. Vetterling, and B. P. Flannery, *Numerical Recipes in C - The Art of Scientific Computing*, Cambridge University Press, 1988, 1992, second edn., URL <http://www.nr.com/>.